Inspection of Industrial Coatings based on Multispectral BTF

Ryosuke Suzuki[1], Fumihiko Sakaue[1], Jun Sato[1], Ryuichi Fukuta[2], Taketo Harada[3] and Kazuhisa Ishimaru[4]

[1]*Nagoya Institute of Technology, Gokiso Showa, Nagoya, Japan*

[2]*DENSO Electronics Corporation, 1-21 Miyama, Shinpukujicho, Okazaki, Japan*

[3]*DENSO Corporation, 1-1, Showa-cho, Kariya, Japan*

[4]*SOKEN Inc., 1-1, Showa-cho, Kariya, Japan*

Keywords: Multispectral BTF, Bidirectional Texture Function, Bidirectional Reflectance Distribution Function, One-class Classifier.

Abstract: In this paper, we propose a method to inspect coatings of industrial products in a factory automation system. The coating of industrial products is important because the coating directly affects the impression of the product, and a large amount of cost is spent on its inspection. Because lots of colors are used in the coating of industrial products, as well as there are various surface treatments such as matte and mirror finishes, the appearance of these products varies hugely. Therefore, it is difficult to obtain the properties of the surfaces by ordinary camera systems, and thus, they are inspected manually in the current system in most cases. In this paper, we present a method of representing surface properties of them, called multispectral BTF, by taking products under narrow-band light from various directions. We also show a method for inspection using a one-class discriminator based on Deep Neural Network using the multispectral BTF. Several experimental results show that our proposed BTF and one-class classifier can inspect various kinds of coating.

1 INTRODUCTION

In recent years, mechanization of the manufacturing process using robots and other devices, so-called factory automation, is widely used, and varieties of technologies have been developed for the systems. In this FA technology, the inspecting processes, whether the product has been created properly or not, are important, as well as the processes of manufacturing and assembling of the products. Therefore, various methods for product inspection have been studied. Especially, image processing and computer vision techniques are widely used(An and Cho, 2015; Perera and Patel, 2019; Bergmann et al., 2019; Schlegl et al., 2017; Akcay et al., 2018; Akçay et al., 2019; Minhas and Zelek, 2019; Dehaene et al., 2019; Bergman and Hoshen, 2019; Zhang et al., 2020) since the technologies require only camera images.

In the product inspection process, not only the functions of the products but also the appearance of them are inspected. Particularly in consumer products, the appearance of the product has a very large impact on the user, strict inspections are required. In addition, because the painting of a product has a strong influence on the preference of the users, many products in recent years have various kinds of painting variations. For example, Fig. 1 shows the paint variations of a vehicle, there are many colors and coatings even for one model as shown in this figure. Furthermore, there is a wide variety of painting methods, such as different amounts of glitter in the paint and different surface finishes, even if the colors are apparently the same.

In order to inspect coatings with such complex properties, the conventional RGB images are not sufficient. In this study, we propose a new method of expressing surface properties, which we call multispectral BTF. This multispectral BTF uses multispectral imaging to measure the detailed color characteristics of a painted surface. We also measure not only color but also detailed reflective characteristics by illuminating the objects with light from various directions. Furthermore, we use deep learning-based methods(He et al., 2016; DOERSCH, 2016; Goodfellow et al., 2014; Radford et al., 2015) to achieve a statistical representation of surface properties. We also show how to construct a one-class discriminator using the proposed features to perform product inspection.

Suzuki, R., Sakaue, F., Sato, J., Fukuta, R., Harada, T. and Ishimaru, K.
Inspection of Industrial Coatings based on Multispectral BTF.
DOI: 10.5220/0010268101560162
In *Proceedings of the 16th International Joint Conference on Computer Vision, Imaging and Computer Graphics Theory and Applications (VISIGRAPP 2021) - Volume 4: VISAPP*, pages 156-162
ISBN: 978-989-758-488-6

Figure 1: Example of color variation of a vehicle.

Note, the product inspection in this study is not to detect partial abnormalities such as scratches and dirt, but to detect overall abnormalities such as differences in products and color errors. The proposed method may be able to deal with partial anomalies as well, but we will not deal with their verification in this paper.

2 REPRESENTATION OF REFLECTANCE PROPERTIES

2.1 Bidirectional Reflectance Distribution Function: BRDF

As described in the introduction, we focus on the reflectance property of the coated surface. Therefore, we first consider the representation of the reflectance property. In order to represent reflectance property effectively, various reflectance models have been studied and proposed(Phong, 1975; Cook and Torrance, 1981). By using theses reflectance models, we can represent light reflectance phenomena by a few parameters. However, these models use strong assumptions to achieve an efficient representation, for example, the surface of the object is rough. On the other hand, the physics-based reflectance models, which based on observation, utilized in recent studies do not contain the assumption. Bidirectional Reflectance Distribution Function (BRDF) is one of the most representative phisics-based reflectance mode(Matt Pharr and Greg Humphreys, 2004).

The BRDF describes distribution of a reflectance ratio $f(\theta_i, \phi_i, \theta_o, \phi_o)$ when a light ray from a direction (θ_i, ϕ_i) to a direction (θ_o, ϕ_o) as shown in Fig.2. The BRDF is 4-dimensional general function, and then the function has many parameters. Therefore, any reflectance property can be represented by this BRDF. However, long time observation is required to obtain the BRDF accurately.

2.2 Bidirectional Texture Function: BTF

By using the BRDF, any object surface property can be represented. However, the BRDF cannot represent

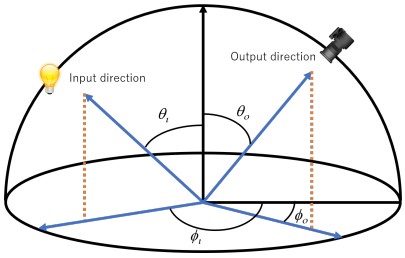

Figure 2: Input light ray and output light ray for BRDF representation.

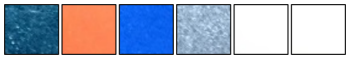

Figure 3: Examples of appearance of the coated object surfaces.

the surface property completely since the objects' surfaces consist of many materials. Figure3 shows examples of coated surfaces. As shown in this figure, the surface coating is made up of multiple materials such as paint, glitter, and so on. Therefore, a single BRDF is not enough to represent surface coating.

To represent the reflectance of surface texture, the Bidirectional Texture Function(Dana et al., 1999) is utilized. As shown in Fig.4, the BTF $f(x, y, \theta_i, \phi_i, \theta_o, \phi_o)$ represents reflectance property, i.e. BRDF, on each point (x, y) by using a 6-dimensional function. Therefore, the BTF represents not only property on a point but also property on a surface.

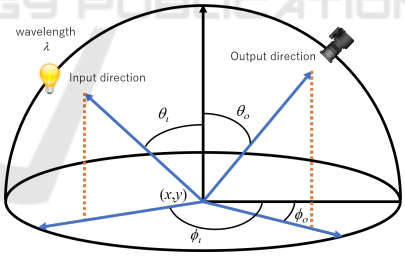

Figure 4: BTF parameters.

3 EFFECTIVE BTF REPRESENTATION WITH MULTISPECTRAL IMAGING

As described above, BTF can represent the reflectance property completely when the distribution of materials on the surface is constant. However, the distribution of materials, i.e. BRDF, in a texture is not necessarily constant on general coatings. Therefore, in order to appropriately represent the properties of textures, a statistical distribution model is required.

Besides, BTF and BRDF are represented by just RGB color in ordinary cases. However, RGB images are not enough to represent reflectance property since the reflectance ratio described by the models strongly depends on the light's wavelength. Therefore, multispectral imaging is required to describe the reflectance property of the surface accurately.

For these reasons, we utilize the multispectral BTF, not taken from RGB images but from multispectral images. The multispectral BTF represents the reflective properties of the paint and coating. Furthermore, we propose a method to represent the statistical properties of the multispectral BTFs using a framework of a GAN(Goodfellow et al., 2014; Radford et al., 2015), which is one of the most representative deep neural networks. By this multispectral BTF representation technique, we will achieve an efficient inspection method for industrial coatings.

3.1 Simplified Multispectral BTF

Firstly, we define the multispectral BTF used in this study. As mentioned above, a 7-dimensional function is required to represent the BTF that includes the wavelength of light. Although this 7-dimensional information may contain complete information for product inspection, it would require a lot of imaging time and complicated imaging devices to acquire all of this information. Therefore, it is not practical to obtain and use the 7-dimensional information completely. Therefore, we define a simplified multispectral BTF for practical use.

In this simplified multispectral BTF, a camera fixed directly above the target is utilized, as shown in Figure 5. Also, the light source is fixed in the direction of longitude ϕ_i and moves only in the direction of latitude θ_i. The light source is equipped with several light sources that can emit narrow-band light, and by switching these light sources turning on and off, we can obtain the reflection characteristics in each band. The information in the BTF can be compressed significantly because this simplified BTF can be expressed as a 4-dimensional function of $f_t(x, y, \theta_i, \lambda)$.

Figure 6 is an example of a simplified BTF. The images at the upper left in each images is an image taken by an ordinary RGB camera. This BTF image is a list of images taken under different latitudes and wavelengths, where the horizontal direction shows the change of wavelength λ and the vertical direction shows the change of latitude θ_i of the light source. Although these images include some similarities in the RGB images, it can be seen that the different BTFs are different features for these images as well.

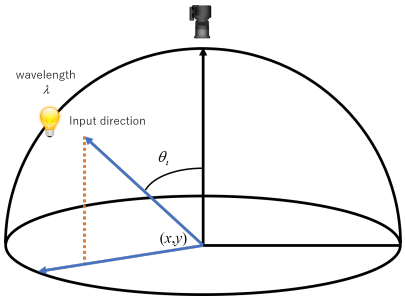

Figure 5: Simplified BTF.

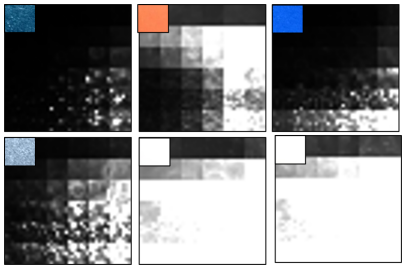

Figure 6: Examples of simplified BTF.

3.2 BTF Representation by GAN

Generative Adversarial Networks, or GAN, are one of the most successful image generation techniques in recent years in the field of deep learning. This GAN achieves higher performance than the method using a single network by competing the network for image generation and the network for discriminating the authenticity of images.Furthermore, various image generation methods derived from the GAN have been proposed, and neural network-based image generation methods have made great progress. In this paper, we use this GAN mechanism and auto-encoder technique to statistically represent the BTF.

Figure 7 shows the outline of the network structure used in this study. In this network, the input BTF image is first mapped into the latent space by an encoder E and then reconstructed as an image by a generator G. This structure is similar to that of a general auto-encoder. However, when a general auto-encoder is used for image mapping and reconstruction, the reconstructed image tends to be smeared. Therefore, the discriminator, which is used in GAN, is introduced in this network to make the reconstructed image more similar to the class of the input image.

Let E denote the encoder that maps the image $\mathbf{X}$ to the latent space and G denotes the generator that reconstructs the image from the latent space. Let D denote the discriminator that discriminates whether the image is from a generator or a real image. In this case, the optimal generator G^* is trained to satisfy the fol-

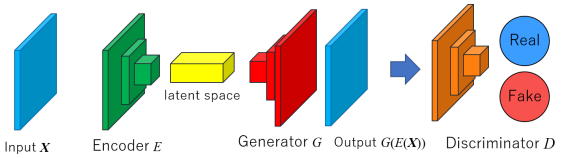

Figure 7: Network architecture for image encoding and decoding.

lowing.

$$G^* = \arg\min_G \max_D V(G,D) \quad (1)$$

$$V(G,D) = \mathbb{E}[\log D(\mathbf{X})] + \mathbb{E}[\log(1-D(G(E(\mathbf{X}))))] + \mathbb{E}[\|\mathbf{X}-G(E(\mathbf{X}))\|] \quad (2)$$

where $\mathbb{E}$ is the expectation value. The first and second terms in $V(G,D)$ are loss functions resulting from the discriminator in GAN. The third term is the image reconstruction error, which is similar to that used in auto-encoder. Thus, by optimizing the discrimination by the discriminator and the image reconstruction error simultaneously, we can reconstruct a more accurate image than using the reconstruction error alone. Thus, the latent space represents the extent of the BTF, such as the distribution of statistical textures and the distribution of reflectance properties.

4 ONE-CLASS CLASIFFIER USING GAN FOR PRODUCT INSPECTION

4.1 Distance from Latent Space in Image Space

We consider a method for determining the input BTF belongs to an objective (registered) class or not. This problem is one-class identification problem using the BTF. By the method described in **3.2**, we can obtain a latent space that can adequately represent the distribution of BTFs. When we consider the latent space as a nonlinear subspace or a manifold in the image space, we can compute the class identity of the input BTF by calculating the distance between the input BTF and the manifold. When an image is mapped and reconstructed, some components that cannot be described in the latent space is lost, and then the distance d_i between the latent space and the input is computed as follows:

$$d_i = \|G(E(\mathbf{X})) - \mathbf{X}\|^2 \quad (3)$$

If the input BTF matches the BTF represented by the GAN, then the reconstructed and the input images are considered similar. Therefore, by calculating the distance d_i, the similarity between the objective class and the input BTF can be measured.

4.2 Image Re-encoder for Classification

Using the encoders and generators described above, we can calculate the similarity between the input image and the registered image class. However, the distance in the image space can easily change due to the inclusion of image noise. In addition, it often happens that the distance in the image space is not so large even if the image pairs look different at glance. Therefore, for stable discrimination, it is necessary to measure distances in the salient feature space, where image features are more prominently represented. Therefore, the reconstructed image is mapped again into the latent space and the distance in the latent space is used for identification.

For this purpose, we learn a new encoder E_2 to map the reconstructed image to the latent space again. The encoder E_2 can be trained by minimizing the following loss so that the map $E_2(G(E(\mathbf{X})))$ of the reconstructed image $G(E(\mathbf{X}))$ is similar to the map $E(\mathbf{X})$ of the input image.

$$\varepsilon_1 = ||E_2(G(E(\mathbf{X}))) - E(\mathbf{X})|| \quad (4)$$

By minimizing this ε_1, the reconstructed image can be mapped to a latent space similar to that by E. This makes it possible to define the distance in the latent space of the input image $\mathbf{X}$ as follows:

$$d_l = \|E_2(G(E(\mathbf{X}))) - E(\mathbf{X})\| \quad (5)$$

By using the distance d_l in this latent space, we can compute the similarity that better reflects the image features.

4.3 Pre-training of Auto-encoder

When computing the BTF similarity using distances in a latent space, the generalization of the latent space, i.e., the ability to represent the BTF, has a significant impact on the discrimination results. This is because if the encoder consists of only images of the registered class, we do not know where the BTF far from the registered class are mapped in the latent space. In this case, a different class of BTFs, the distances inside the latent space happen to be close together. In order to solve these problems, it is important to be able to separate different classes within the latent space.Therefore, in this study, we pre-train this encoder to represent various images using a discrimination problem.

Let us consider the case when we have an image set $\mathbf{X}_i$ that belongs to class i. If $\mathbf{X}_i$ is classified based

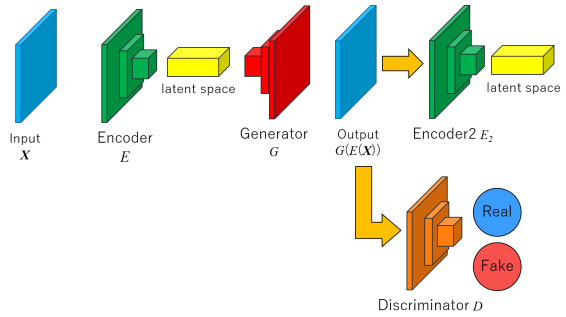

Figure 8: Network architecture.

on the $\mathbf{z}_i$, which is mapped to the latent space using the encoder E, the encoder E can represent various classes of images appropriately. Therefore, we train E and C by connecting a new classification network C connected to the encoder E and minimizing its output with the following cross-entropy error ε_2.

$$\varepsilon_2 = -\sum_k t_k C(E(X_i)) \tag{6}$$

where t_k is a correct label that is 1 when $k = i$ and 0 otherwise. In this way, we can improve the representation of E by learning the Encoder E in advance using discrimination problems.

4.4 Product Inspection Network

We summarize the network used in this study for product coating inspection. Figure 8 summarizes the network structure used in the similarity computation. By using this network, it is possible to compute the distance d_i between the input image and the latent space in the image space, and the distance d_l in latent space. Therefore, the following distances, which are integrated from these distances, are used as indices for product inspection.

$$d = (1-w)d_i + wd_l \tag{7}$$

By Using this distance d, we determine whether the input image is proper (1) or not (0) by the following threshold processing.

$$\delta(\mathbf{X}) = \begin{cases} 1 & d \leq \theta \\ 0 & \text{otherwise} \end{cases} \tag{8}$$

5 EXPERIMENTAL RESULTS

5.1 Environment

We show several experimental results to confirm the effectiveness of the proposed method. In these experiments, we measured the BTF of actual industrial products and checked whether it was possible to discriminate between registered products and other products using the proposed one-class classifier. There are various kinds of coatings on these products, and we used 107 products in our experiments. We chose several products as known products in these 107 products, and the encoder E was pre-trained by using them. We also chose one product as a registered product that we wanted to identify, and we trained a generator G and an encoder E_2 by this. Using the trained G, E, and E_2, we tested whether the proposed one-class discriminator can discriminate between registered products and the unknown products. For comparison, experiments were conducted with several features as well as proposed multispectral BTFs. The features used for the comparison are ordinary BTF, multispectral images and RGB images. The encoders E and E_2, and the generator G were trained by using the features in the same way for multispectral BTF. Note that the RGB and multispectral images were taken under a single light source. Table 1 summarizes the specification of the experiment in table 1. The detailed network structure of the encoder, generator and discriminator is shown in Fig.9.

Table 1: Specification of the experiment.

# of classes	107
image block size	32×32
# of wavelength	6
# of latitude	7
# of images for each class	600

5.2 Results

First, we experimented with checking whether the proposed one-class discriminator can be used to identify similar products. In this experiment, we chose the 4 white products shown in Figure 10. As shown in this figure, these products are very similar to each other in the RGB image. One of these products is registered. So, G and E_2 were trained by the registered class. The other is used as the test class. We checked whether the registered product and the test product could be classified. Figure 11 is an image of a product taken by an RGB camera. Also, Figure 11 shows the results of measuring the multispectral BTF from each product. These images show that even though the products are very similar in the RGB images, they have different features in the multispectral-BTF.

Figure 12 shows ROC (Receiver Operating Characteristics) curve, which is drawn from a set False Acceptance Rate (FAR) and True Accept Rate (TAR) with varying the threshold. This graph shows the classifier's characteristics, and when the curve close to

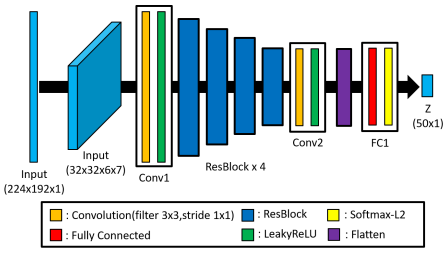

(a) encoder

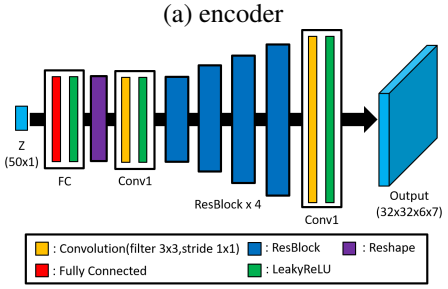

(b) generator

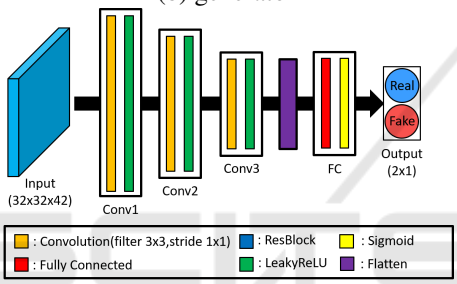

(c) discriminator

Figure 9: Detailed network architectures for (a)encoder, (b)generator and (c)discriminator.

(a) (b) (c) (d)

Figure 10: Target products taken by RGB camera.

the upper left, the characteristics become better. The worst property is when the curve is a diagonal line. When the multispectral BTF is used, the ROC curve is surprisingly closer to the upper left. In contrast, the ROC curve is closer to the diagonal in the case of the other features are used, which shows a clear inferiority in performance compared to the case of multispectral BTF. The area under the curve (AUC) in each case are shown in table2, where AUC is the overall evaluation of ROC, from 1 in the best case to 0.5 in the worst case. The effectiveness of multispectral BTF can be confirmed by the fact that better results were obtained with multispectral BTF in table2 as well. These results confirmed the effectiveness of the multispectral BTF in the inspection of coatings.

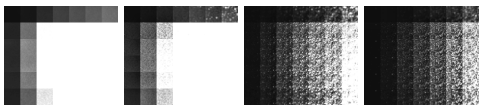

(a) (b) (c) (d)

Figure 11: Examples of multispectral BTF for each product.

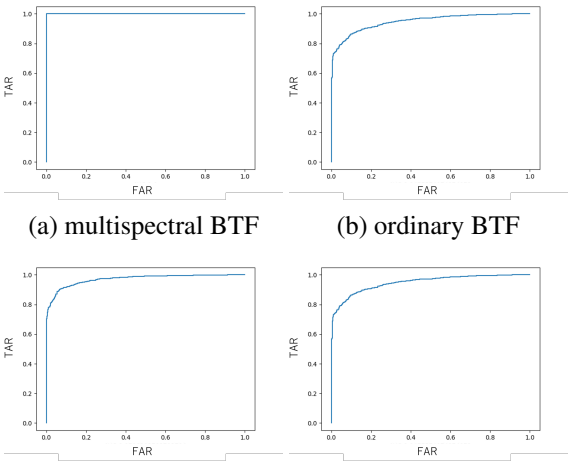

(a) multispectral BTF (b) ordinary BTF

(c) multispectral image (d) RGB image

Figure 12: ROC curves: (a) shows ROC for multispectral BTF, (b) is for ordinary BTF, (c) is for multispectral image and (d) is for RGB image.

Table 2: Area under curve (AUC) for each ROC curve.

features	AUC
mult-BTF	1.00
ordinary BTF	0.96
mult-image	0.97
RGB image	0.94

Next, we present the results of an exhaustive experiment. In this experiment, we used half of the 107 classes for pre-training in the encoder E. We chose a class that was not used for pre-training and used it as the registered class. The other classes that were not used in either of the pre-training registrations were used as test classes to confirm they could be classified into the registered class. This operation was repeated 25 times while varying the registered class. The ROC curves obtained in the experiments are shown in Figure13. The AUCs for each result are also shown in Tab.3

Table 3: Area under curve (AUC) for each ROC curve.

features	AUC
mult-BTF	0.98
ordinary BTF	0.98
mult-image	0.96
RGB image	0.92

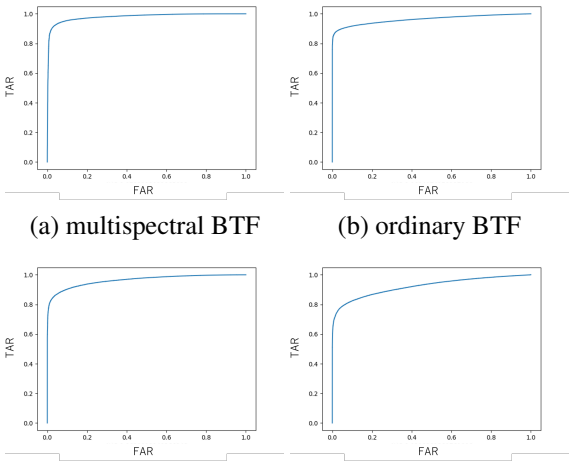

(a) multispectral BTF (b) ordinary BTF

(c) multispectral image (d) RGB image

Figure 13: ROC curves for (a) multispectral BTF, (b) ordinary BTF, (c) RGB image and (d) multispectral image.

In these results, we can confirm that the best discrimination results are obtained with the proposed method. Thesed results indicate that the classification performance by the proposed method is higher than other results using the other features. These results confirm that the multispectral BTF proposed in this paper can adequately represent the coating characteristics of industrial products.

6 CONCLUSION

In this study, a multispectral BTF was proposed to represent the reflective properties of fine surfaces for the inspection of industrial products. In addition, a method for 1-class identification using deep learning for product inspection using multispectral BTF is presented. Furthermore, one-class discrimination experiments of actual products were conducted using the proposed method, and it was confirmed that the multispectral BTF is effective for the inspection of coatings. In future work, we plan to study not only the identification of products but also a method for detecting partial abnormalities such as scratches and dirt.

REFERENCES

Akcay, S., Atapour-Abarghouei, A., and Breckon, T. P. (2018). Ganomaly: Semi-supervised anomaly detection via adversarial training. In *Asian conference on computer vision*, pages 622–637. Springer.

Akçay, S., Atapour-Abarghouei, A., and Breckon, T. P. (2019). Skip-ganomaly: Skip connected and adversarially trained encoder-decoder anomaly detection. In *2019 International Joint Conference on Neural Networks (IJCNN)*, pages 1–8. IEEE.

An, J. and Cho, S. (2015). Variational autoencoder based anomaly detection using reconstruction probability. *Special Lecture on IE*, 2(1):1–18.

Bergman, L. and Hoshen, Y. (2019). Classification-based anomaly detection for general data. In *International Conference on Learning Representations*.

Bergmann, P., Löwe, S., Fauser, M., Sattlegger, D., and Steger, C. (2019). Improving unsupervised defect segmentation by applying structural similarity to autoencoders.

Cook, R. L. and Torrance, K. E. (1981). A reflectance model for computer graphics. *SIGGRAPH Comput. Graph.*, 15(3):307–316.

Dana, K. J., van Ginneken, B., Nayar, S. K., and Koenderink, J. J. (1999). Reflectance and texture of real-world surfaces. *ACM Trans. Graph.*, 18(1):1–34.

Dehaene, D., Frigo, O., Combrexelle, S., and Eline, P. (2019). Iterative energy-based projection on a normal data manifold for anomaly localization. In *International Conference on Learning Representations*.

DOERSCH, C. (2016). Tutorial on variational autoencoders. *stat*, 1050:13.

Goodfellow, I., Pouget-Abadie, J., Mirza, M., Xu, B., Warde-Farley, D., Ozair, S., Courville, A., and Bengio, Y. (2014). Generative adversarial nets. In *Advances in neural information processing systems*, pages 2672–2680.

He, K., Zhang, X., Ren, S., and Sun, J. (2016). Deep residual learning for image recognition. In *Proceedings of the IEEE Conference on Computer Vision and Pattern Recognition (CVPR)*.

Matt Pharr and Greg Humphreys (2004). *Physically Based Rendering: From Theory to Implementation*. Morgan Kaufmann.

Minhas, M. S. and Zelek, J. S. (2019). Anomaly detection in images. *CoRR*, abs/1905.13147.

Perera, P. and Patel, V. M. (2019). Learning deep features for one-class classification. *IEEE Transactions on Image Processing*, 28(11):5450–5463.

Phong, B. T. (1975). Illumination for computer generated pictures. *Commun. ACM*, 18(6):311–317.

Radford, A., Metz, L., and Chintala, S. (2015). Unsupervised representation learning with deep convolutional generative adversarial networks. *arXiv preprint arXiv:1511.06434*.

Schlegl, T., Seeböck, P., Waldstein, S. M., Schmidt-Erfurth, U., and Langs, G. (2017). Unsupervised anomaly detection with generative adversarial networks to guide marker discovery. In *International conference on information processing in medical imaging*, pages 146–157. Springer.

Zhang, J., Xie, Y., Liao, Z., Pang, G., Verjans, J., Li, W., Sun, Z., He, J., Li, Y., Shen, C., et al. (2020). Viral pneumonia screening on chest x-ray images using confidence-aware anomaly detection. *arXiv: 2003.12338*.